$K\beta/K\alpha$ intensity ratios for x-ray production by fast deuterons, α particles, and carbon ions*

T. K. Li and R. L. Watson

Department of Chemistry and Cyclotron Institute, Texas A&M University, College Station, Texas 77843

(Received 12 October 1973)

Systematic measurements of $K\beta/K\alpha$ intensity ratios have been carried out for a wide range of targets ($19 \leq Z \leq 47$) using 2.35- to 12.5-MeV/amu deuterons, α particles, and carbon ions. Radiative-transition probability ratios were calculated for various L- and M-shell vacancy configurations using Hartree-Fock-Slater wave functions. Employing information previously obtained on simultaneous K- plus L-shell ionization, the velocity dependence of the simultaneous K- plus M-shell ionization probability was characterized and compared with the velocity dependence expected for ionization by direct Coulomb excitation.

I. INTRODUCTION

In a number of recent spectral measurements of K x rays arising from heavy-charged-particle bombardments, it has been observed that the $K\beta/K\alpha$ intensity ratios are considerably different from those obtained with more conventional methods of x-ray production. For example, the relative intensities of $K\alpha$ and $K\beta$ x rays emitted from various targets following ionization by nitrogen ions,[1] oxygen ions,[2] and fission fragments[3] are not the same as those observed in association with ionization produced by photons, electrons, and as a result of radioactive decay. These large variations in the $K\beta/K\alpha$ intensity ratios are yet another indication of the influence of the excited-state configuration on the x-ray emission process. Since the $K\alpha$ x-ray transitions originate from $2p$ levels and the predominant $K\beta$ x-ray transitions originate from $3p$ levels, it is to be expected that the relative intensities of these transitions should depend rather sensitively on the number of L- and M-shell vacancies in existence at the time of x-ray emission.

The present study was undertaken for the purpose of systematically comparing $K\beta/K\alpha$ intensity ratios characteristic of x-ray production by light and heavy ions with those which characterize x-ray production by other means. Measurements have been carried out for a wide range of elements extending from $Z = 19$ to $Z = 47$ using 2.35 to 12.5-MeV/amu deuterons, α particles, and carbon ions. In addition, Hartree-Fock-Slater (HFS) calculations of $K\beta/K\alpha$ intensity ratios for various L- and M-shell vacancy configurations have been performed in order to ascertain the extent to which the experimental results may be understood in terms of simultaneous K- plus L- and M-shell ionization.

II. EXPERIMENTAL METHODS

The experimental techniques used in the present study of $K\beta/K\alpha$ x-ray intensity ratios were basically the same as those described previously.[4] Deuterons and α particles having energies of 2.88, 6.25, 7.50, and 12.50 MeV/amu, and carbon ions of 2.35, 3.75, 6.25, and 8.33 MeV/amu were used. The targets were all prepared by vacuum evaporation and ranged from 20 to 135 $\mu g/cm^2$ in effective thickness. A list of the targets used is presented in Table I.

A 30-mm^2 × 3-mm Si(Li) x-ray spectrometer giving an energy resolution of 240 eV (full width

TABLE I. Targets used in the $K\beta/K\alpha$ x-ray intensity ratio measurements.

Target	Effective [a] thickness ($\mu g/cm^2$)	Chemical form	Target backing
K	20	KBr	0.153 mg/cm^2 Al
Ca	35	CaF_2	0.52 mg/cm^2 Mylar
Sc	39	Sc_2O_3	1.72 mg/cm^2 Al
Ti	35	metal	0.52 mg/cm^2 Mylar
V	100	metal	0.52 mg/cm^2 Mylar
Cr	81	metal	1.72 mg/cm^2 Al
Mn	71	metal	1.72 mg/cm^2 Al
Fe	41	metal	0.52 mg/cm^2 Mylar
Co	59	metal	0.52 mg/cm^2 Mylar
Ni	49	metal	0.52 mg/cm^2 Mylar
Cu	96	metal	0.52 mg/cm^2 Mylar
Zn	135	metal	0.52 mg/cm^2 Mylar
Ge	106	elemental	0.52 mg/cm^2 Mylar
Se	91	elemental	0.52 mg/cm^2 Mylar
Br	41	KBr	0.153 mg/cm^2 Al
Mo	89	metal	0.153 mg/cm^2 Al
Ag	72	metal	0.52 mg/cm^2 Mylar

[a] Account has been taken of the 45° target inclination angle.

at half-maximum at 6.4 keV) was located 19.0 cm from the target at 90° to the incident beam. The spectrometer system was separated from the target chamber by a 4.7 mg/cm^2 beryllium window. Sample Fe K x-ray spectra obtained with deuterons, α particles, and carbon ions are shown in Fig. 1. All of the x-ray spectra were carefully analyzed with the least-squares peak-fitting program of Rugge *et al.*[5] A fit to the experimental data points was achieved in each case by representing the $K\alpha$ and $K\beta$ peak shapes with Gaussian functions having exponential tails and by allowing the widths, means, and areas of the calculated peaks, and three parameters specifying a quadratic background, all to vary in combination until an optimized set was obtained by the method of least squares.

An efficiency calibration of the Si(Li) x-ray spectrometer was accomplished over the energy range 5.4–59.5 keV by counting IAEA standard sources[6] of ^{57}Co, ^{54}Mn, ^{137}Cs, and ^{241}Am under vacuum with the sources located at the target position. Corrections for x-ray absorption in the 17.5 mg/cm^2 polyethylene layer which covered the sources were made for photons of energies less than 14.4 keV. An efficiency calibration at 3.3 keV was obtained by counting NpM x-rays from a thin, uncovered ^{241}Am source, in the same manner as described above. In all cases, conversion from source disintegration rate to x-ray photons per second was made using the percentage-per-disintegration values recommended by Hansen *et al.*[7] The reliability of the *relative* efficiency curve resulting from these measurements is believed to be of the order of ±2%.

III. RESULTS

The results of the present $K\beta/K\alpha$ intensity ratio measurements are presented in Tables II–IV. They have been corrected for absorption and for detector efficiency. The errors listed in these tables are the root-mean-square deviations from three or more independent measurements. These error values do not include the 2% uncertainty in the relative efficiency of the spectrometer system. The absolute values of the $K\beta/K\alpha$ ratios listed for K, Ca, and Sc are subject to an additional error ~10% associated with the difficulty of accurately extracting the individual intensities of their closely overlapping $K\beta/K\alpha$ peaks.

A relative comparison of the $K\beta/K\alpha$ intensity ratios obtained with 6.25-MeV/amu deuterons, α particles, and carbon ions is shown in Fig. 2. In

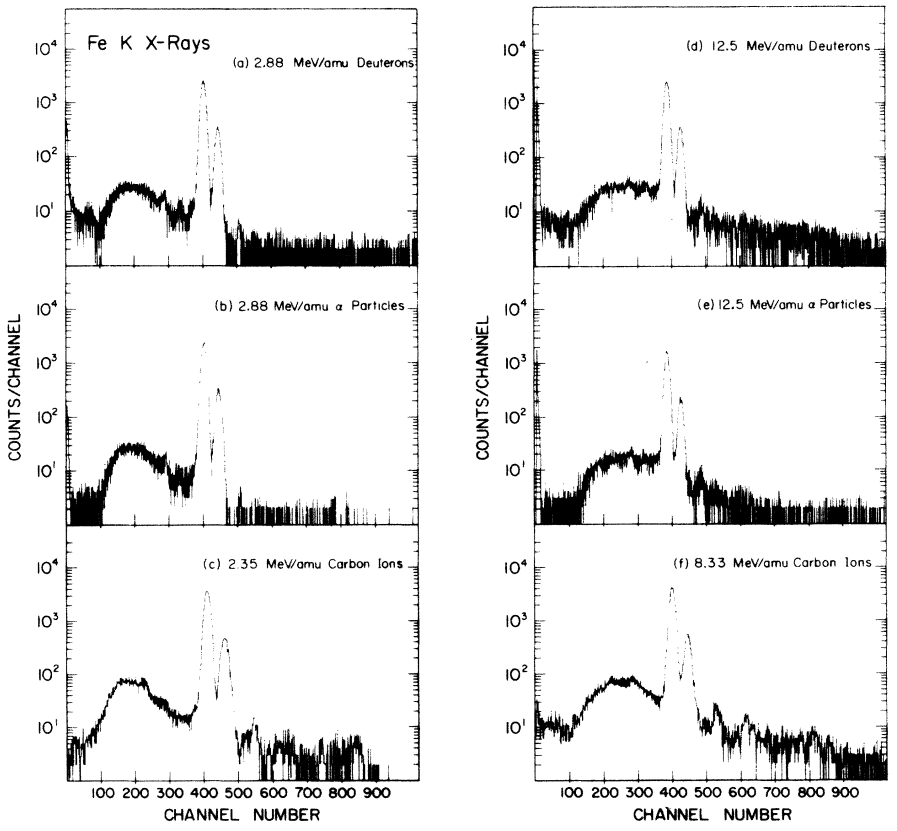

FIG. 1. Sample K x-ray spectra for Fe obtained in bombardments with deuterons, α particles, and carbon ions, at the lowest and highest projectile energies used in this study.

TABLE II. $K\beta/K\alpha$ intensity ratios for x-ray production by deuterons. The listed errors represent the *relative* uncertainty in the measurements. An additional ±2% absolute uncertainty is associated with the efficiency correction.

	2.88 MeV/amu	6.25 MeV/amu	7.50 MeV/amu	12.50 MeV/amu
K [a]	0.138 ± 0.002	0.139 ± 0.002	0.138 ± 0.002	0.137 ± 0.006
Ca [a]	0.135 ± 0.005	0.134 ± 0.001	0.132 ± 0.002	0.133 ± 0.002
Sc [a]	0.133 ± 0.002	0.132 ± 0.001	0.132 ± 0.002	0.131 ± 0.002
Ti	0.127 ± 0.003	0.126 ± 0.002	0.126 ± 0.002	0.127 ± 0.001
V	0.128 ± 0.001	0.128 ± 0.002	0.129 ± 0.001	0.129 ± 0.001
Cr	0.129 ± 0.002	0.129 ± 0.002	0.130 ± 0.002	0.129 ± 0.002
Mn	0.129 ± 0.002	0.130 ± 0.001	0.130 ± 0.002	0.130 ± 0.004
Fe	0.127 ± 0.002	0.126 ± 0.002	0.126 ± 0.001	0.127 ± 0.002
Co	0.128 ± 0.003	0.127 ± 0.002	0.128 ± 0.001	0.128 ± 0.002
Ni	0.134 ± 0.001	0.133 ± 0.001	0.133 ± 0.001	0.132 ± 0.001
Cu	0.135 ± 0.002	0.134 ± 0.001	0.134 ± 0.002	0.134 ± 0.001
Zn	0.138 ± 0.002	0.138 ± 0.002	0.137 ± 0.001	0.139 ± 0.003
Ge	0.149 ± 0.002	0.147 ± 0.002	0.147 ± 0.003	0.148 ± 0.003
Se	0.162 ± 0.002	0.162 ± 0.001	0.163 ± 0.001	0.165 ± 0.002
Br	0.164 ± 0.003	0.165 ± 0.002	0.164 ± 0.004	0.166 ± 0.001
Mo	0.192 ± 0.002	0.195 ± 0.002	0.197 ± 0.004	0.198 ± 0.003
Ag	0.203 ± 0.004	0.204 ± 0.006	0.208 ± 0.004	0.208 ± 0.006

[a] An additional ±10% absolute uncertainty associated with the deconvolution of the closely overlapping $K\alpha$ and $K\beta$ peaks applies to these cases.

TABLE IV. $K\beta/K\alpha$ intensity ratios for x-ray production by carbon ions. The listed errors represent the *relative* uncertainty in the measurements. An additional ±2% absolute uncertainty is associated with the efficiency correction.

	2.35 MeV/amu	3.75 MeV/amu	6.25 MeV/amu	8.33 MeV/amu
K [a]	0.187 ± 0.005	0.180 ± 0.004	0.178 ± 0.004	0.174 ± 0.007
Ca [a]	0.175 ± 0.003	0.168 ± 0.003	0.159 ± 0.002	0.155 ± 0.002
Sc [a]	0.168 ± 0.003	0.163 ± 0.002	0.160 ± 0.001	0.158 ± 0.002
Ti	0.162 ± 0.004	0.154 ± 0.003	0.143 ± 0.002	0.138 ± 0.003
V	0.156 ± 0.003	0.152 ± 0.003	0.142 ± 0.002	0.141 ± 0.003
Cr	0.152 ± 0.003	0.145 ± 0.003	0.139 ± 0.004	0.138 ± 0.002
Mn	0.153 ± 0.002	0.146 ± 0.001	0.140 ± 0.001	0.140 ± 0.002
Fe	0.153 ± 0.001	0.147 ± 0.001	0.142 ± 0.002	0.138 ± 0.003
Co	0.154 ± 0.001	0.146 ± 0.001	0.143 ± 0.002	0.138 ± 0.002
Ni	0.162 ± 0.001	0.151 ± 0.002	0.148 ± 0.001	0.142 ± 0.002
Cu	0.165 ± 0.002	0.156 ± 0.001	0.146 ± 0.002	0.143 ± 0.001
Zn	0.164 ± 0.001	0.160 ± 0.003	0.151 ± 0.001	0.149 ± 0.003
Ge	0.172 ± 0.001	0.168 ± 0.001	0.163 ± 0.002	0.158 ± 0.001
Se	0.179 ± 0.002	0.176 ± 0.001	0.173 ± 0.002	0.171 ± 0.001
Br	0.178 ± 0.004	0.176 ± 0.004	0.174 ± 0.002	0.173 ± 0.004
Mo	0.210 ± 0.003	0.207 ± 0.004	0.204 ± 0.005	0.202 ± 0.005
Ag	0.222 ± 0.003	0.221 ± 0.005	0.219 ± 0.005	0.216 ± 0.007

[a] An additional ±10% absolute uncertainty associated with the deconvolution of the closely overlapping $K\alpha$ and $K\beta$ peaks applies to these cases.

this figure, R_α/R_d and R_c/R_d are plotted as a function of target atomic number, where R_d, R_α, and R_c are the $K\beta/K\alpha$ intensity ratios for deuterons, α particles, and carbon ions, respectively. It is seen that the R_c/R_d data deviate considerably from unity (dashed line) and that the deviations increase with decreasing target atomic number (from ~5% for $Z=47$ to ~30% for $Z=19$). The R_α/R_d data, on the other hand, appear to be only slightly greater than unity (~2%) and do not vary with atomic number. This behavior apparently reflects the relative importance of simultaneous L-shell ionization produced by the three types of charged particles in K-shell ionizing collisons. One also notes in Table IV that the $K\beta/K\alpha$ intensity ratios for carbon ion excitation increase with decreasing projectile velocity. This energy dependence will be investigated further in Sec. IV.

TABLE III. $K\beta/K\alpha$ intensity ratios for x-ray production by alpha particles. The listed errors represent the *relative* uncertainty in the measurements. An additional ±2% absolute uncertainty is associated with the efficiency correction.

	2.88 MeV/amu	6.25 MeV/amu	7.50 MeV/amu	12.50 MeV/amu
K [a]	0.142 ± 0.001	0.141 ± 0.004	0.140 ± 0.001	0.138 ± 0.009
Ca [a]	0.139 ± 0.001	0.136 ± 0.002	0.135 ± 0.003	0.134 ± 0.001
Sc [a]	0.137 ± 0.002	0.136 ± 0.001	0.137 ± 0.003	0.137 ± 0.002
Ti	0.129 ± 0.002	0.128 ± 0.001	0.128 ± 0.002	0.130 ± 0.003
V	0.128 ± 0.002	0.129 ± 0.002	0.131 ± 0.003	0.131 ± 0.003
Cr	0.128 ± 0.001	0.130 ± 0.001	0.130 ± 0.002	0.130 ± 0.002
Mn	0.129 ± 0.002	0.130 ± 0.002	0.131 ± 0.001	0.131 ± 0.003
Fe	0.129 ± 0.002	0.128 ± 0.002	0.129 ± 0.002	0.129 ± 0.002
Co	0.130 ± 0.001	0.129 ± 0.003	0.130 ± 0.002	0.131 ± 0.001
Ni	0.135 ± 0.001	0.134 ± 0.003	0.133 ± 0.001	0.132 ± 0.001
Cu	0.137 ± 0.001	0.136 ± 0.002	0.136 ± 0.001	0.137 ± 0.002
Zn	0.139 ± 0.003	0.140 ± 0.002	0.139 ± 0.001	0.142 ± 0.002
Ge	0.148 ± 0.002	0.149 ± 0.004	0.150 ± 0.001	0.150 ± 0.001
Se	0.164 ± 0.001	0.163 ± 0.004	0.163 ± 0.001	0.165 ± 0.001
Br	0.166 ± 0.003	0.164 ± 0.002	0.165 ± 0.003	0.166 ± 0.002
Mo	0.193 ± 0.003	0.197 ± 0.002	0.198 ± 0.002	0.199 ± 0.003
Ag	0.203 ± 0.004	0.206 ± 0.006	0.210 ± 0.005	0.210 ± 0.006

[a] An additional ±10% absolute uncertainty associated with the deconvolution of the closely overlapping $K\alpha$ and $K\beta$ peaks applies to these cases.

IV. DISCUSSION

Systematic experimental determinations of $K\beta/K\alpha$ x-ray-intensity ratios have been reported for photon and bremsstrahlung irradiation by Slivinsky and Ebert,[8] McCrary *et al.*,[9] and Salem *et al.*,[10] for radioactive decay by Hansen *et al.*,[11] and for electron excitation by Mistry and Quarles.[12] Their results are plotted as a function of atomic number (for $Z \leq 50$) in Fig. 3. It is seen that, except for the radioactive decay results of Hansen *et al.*, the data are in excellent agreement. Theoretical predictions of radiative transition probabilities for the K-shell in elements of $Z < 50$ have been reported by Scofield[13] and by Rosner and Bhalla.[14] The results of their calculations (which agree within 5%) are shown by the solid line in Fig. 3. Rather large and unexplained deviations between theory and experiment are found.

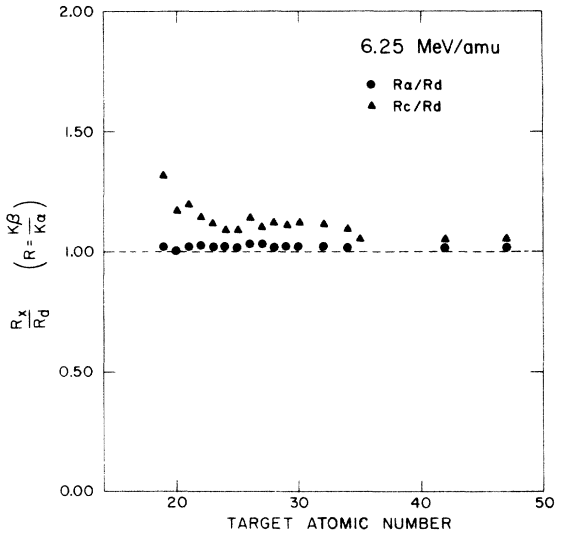

FIG. 2. Target atomic-number dependence of R_α/R_d and R_c/R_d at 6.25 MeV/amu projectile energy, where R_d, R_α, and R_c are $K\beta/K\alpha$ intensity ratios obtained with deuterons, α particles, and carbon ions, respectively.

A comparison of the $K\beta/K\alpha$ intensity ratios for x-ray emission induced by 6.25-MeV/amu deuterons, α particles, and carbon ions with the photon and bremsstrahlung data mentioned above is shown in Fig. 4. The dashed curve in this figure shows the theoretical predictions of Scofield.[13] It is seen that the $K\beta/K\alpha$ intensity ratios for x-ray production by carbon ions are systematically larger than those for x-ray production by photons and bremsstrahlung, which is qualitatively consistent with the fact that multiple L-shell ionization is highly probable in heavy ion-atom collisions.[15] The $K\beta/K\alpha$ intensity ratios for x-ray production by deuterons and α particles, on the other hand, are slightly lower than the photon and bremsstrahlung values in the region of $Z=22$ to 30. Possibly, this behavior indicates that in the case of light ions simultaneous M-shell ionization is the dominant factor affecting the $K\beta/K\alpha$ intensity ratios.

In an effort to determine how sensitive $K\beta$ and $K\alpha$ transition probabilities (per electron) are to the number of L- and M-shell vacancies, we have carried out calculations of the relevant dipole matrix elements for various L- and M-shell vacancy configurations using numerical nonrelativistic wave functions and transition energies computed with the HFS program of Herman and Skillman.[16] In these calculations the electrons were represented by single-particle wave functions in a central potential and no relativistic corrections or retardation effects were included. The transition energies were obtained from the differences

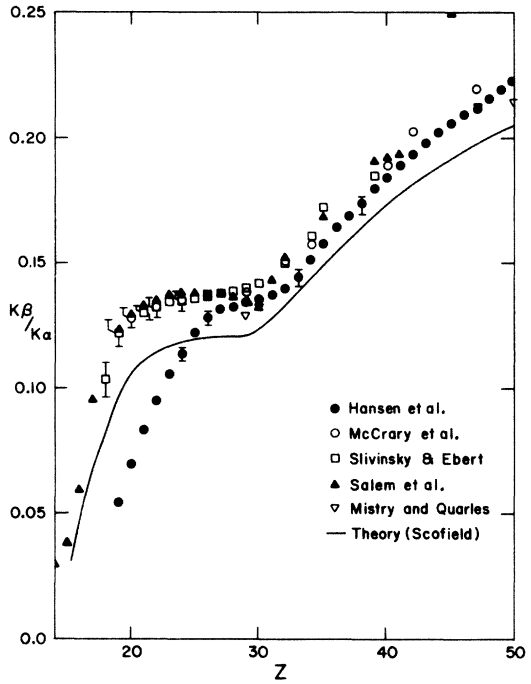

FIG. 3. $K\beta/K\alpha$ x-ray intensity ratio as a function of atomic number. Experimental data are taken from the work previously reported by Mistry and Quarles (Ref. 12), Slivinsky and Ebert (Ref. 8), Hansen *et al.* (Ref. 11), McCrary *et al.* (Ref. 9), and Salem *et al.* (Ref. 10). The solid curve is the theoretical prediction from Scofield's calculations (Ref. 13).

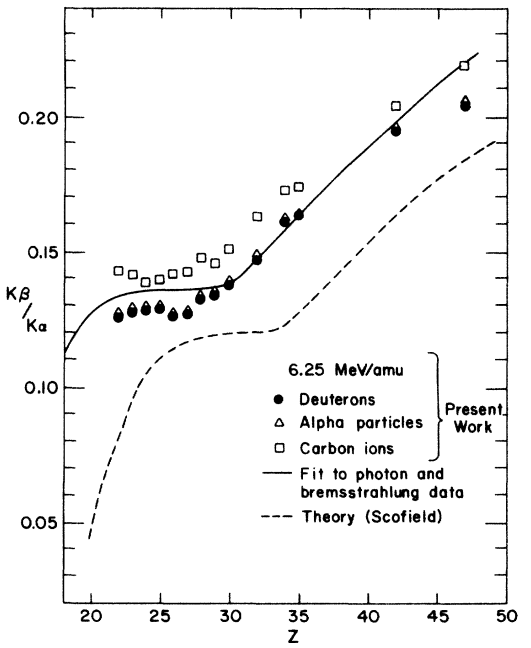

FIG. 4. $K\beta/K\alpha$ x-ray intensity ratios resulting from 6.25-MeV/amu deuteron, α particle, and carbon ion bombardments as a function of target atomic number.

of the total energies of the initial and final states as calculated with the HFS program. For example, the Ti $K\alpha$ and $K\beta$ x-ray transition probabilities for an initial-state configuration consisting of a single $1s$ vacancy plus a single $2p$ vacancy ($1s^{-1}2p^{-1}$) can be expressed, respectively, as

$$I_{1s^{-1}2p^{-1}}(K\alpha) = A(E_{1s^{-1}2p^{-1}} - E_{2p^{-2}})^3 \times |\langle \psi_{2p^{-2}}(1s)|\bar{r}|\psi_{1s^{-1}2p^{-1}}(2p)\rangle|^2 \quad (1)$$

and

$$I_{1s^{-1}2p^{-1}}(K\beta) = A(E_{1s^{-1}2p^{-1}} - E_{2p^{-1}3p^{-1}})^3 \times |\langle \psi_{2p^{-1}3p^{-1}}(1s)|\bar{r}|\psi_{1s^{-1}2p^{-1}}(3p)\rangle|^2.$$

Here, the E's are the total energies for the specified configurations and $A = N\frac{4}{3}(e^2/\hbar^4c^3)$, where N is the number of electrons available to participate in the transition. Similar calculations have recently been performed by Bhalla, Folland, and Hein[17] and by Bhalla[18] for multiply ionized neon and argon atoms. Further details of the present transition probability calculations are given in Ref. 19. Calculated Ti ($Z=22$) $K\alpha$ and $K\beta$ x-ray transition widths *per electron* for various initial-state vacancy configurations are listed in Table V. The present results for the $1s^{-1}$ case agree with the results of the more rigorous calculations by Scofield[13] to within 12% for the total K x-ray emission rate and to within 1.4% for the $K\beta/K\alpha$ intensity ratio. It is seen in Table V that the $K\alpha$ and $K\beta$ transition widths per electron both *increase* as $2p$ and $3p$ electrons are removed. The $K\alpha$ widths change by 21% and 15% upon removal of five $2p$- and five $3p$-electrons, respectively. The $K\beta$ widths change by as much as 76% and 31% upon removal of five $2p$- and five $3p$-electrons, respectively. Thus, it is found that the $K\alpha$ and $K\beta$ transition widths per electron are considerably more sensitive to the presence of $2p$ vacancies than to the presence of $3p$ vacancies. The calculated $K\beta/K\alpha$ intensity ratios for Ti are shown in Fig. 5 as a function of the initial vacancy-state configuration. One notices that the $K\beta/K\alpha$ intensity ratio is a strongly increasing function of the number of $2p$ vacancies and a somewhat more slowly decreasing function of the number of $3p$ vacancies. The dashed and dot-dashed curve in Fig. 5 show the $K\beta/K\alpha$ intensity ratios obtained by simply scaling the $K\beta/K\alpha$ intensity ratio for a $1s^{-1}$ initial state by the appropriate factors to account for the missing $2p$ and $3p$ electrons; for example,

$$K\beta/K\alpha(1s^{-1}2p^{-1}) \simeq \tfrac{6}{5}K\beta/K\alpha(1s^{-1}),$$

$$K\beta/K\alpha(1s^{-1}3p^{-2}) \simeq \tfrac{4}{6}K\beta/K\alpha(1s^{-1}),$$

etc. This procedure has been used by Larkins[20] to estimate fluorescence yields for multiply ionized argon atoms. The scaled $K\beta/K\alpha$ intensity ratios are 46% and 29% lower than the calculated

TABLE V. Calculated $K\alpha$ and $K\beta$ x-ray transition widths *per electron* for Ti.

Ion configuration	$\Gamma_{K\alpha}$ (eV)	$\Gamma_{K\beta}$ (eV)
$1s^{-1}$	0.1872	0.0216
$1s^{-1}2p^{-1}$	0.1947	0.0246
$1s^{-1}2p^{-2}$	0.2023	0.0277
$1s^{-1}2p^{-3}$	0.2102	0.0310
$1s^{-1}2p^{-4}$	0.2182	0.0345
$1s^{-1}2p^{-5}$	0.2263	0.0381
$1s^{-1}3p^{-1}$	0.1876	0.0228
$1s^{-1}3p^{-2}$	0.0881	0.0240
$1s^{-1}3p^{-3}$	0.1886	0.0254
$1s^{-1}3p^{-4}$	0.1892	0.0267
$1s^{-1}3p^{-5}$	0.1900	0.0282

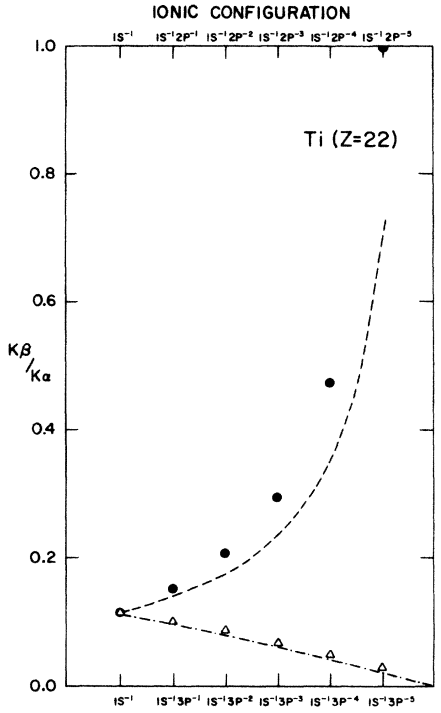

FIG. 5. Calculated (HFS) $K\beta/K\alpha$ intensity ratio as a function of the initial inner-shell vacancy configuration. The solid circles are $K\beta/K\alpha$ intensity ratios corresponding to configurations listed at the top of the graph and the open triangles are $K\beta/K\alpha$ intensity ratios corresponding to configurations listed at the bottom of the graph. The dashed and dot-dashed curves are $K\beta/K\alpha$ ratios obtained by scaling the $K\beta/K\alpha$ ratio for the $1s^{-1}$ configuration to account for the missing $2p$ and $3p$ electrons, respectively.

$K\beta/K\alpha$ intensity ratios for initial-state configurations having five $2p$ and five $3p$ vacancies, respectively. Thus, it is apparent that while the scaling procedure can lead to large errors in estimating such quantities as $K\beta/K\alpha$ intensity ratios, transition widths, and fluorescence yields for *extreme* states of multiple L-shell ionization, it is nevertheless capable of providing fairly reasonable estimates for configurations involving multiple M-shell ionization.

The complexity of the task involved in relating measured $K\beta/K\alpha$ intensity ratios to theoretical predictions based upon theories describing the ionization process can be understood from the following considerations. Experimental values of $K\beta/K\alpha$ intensity ratios represent averages of relative $K\alpha$ and $K\beta$ transition probabilities over all configurations contributing to the x-ray yield and may be expressed as

$$(I_{K\beta}/I_{K\alpha})_{\text{expt}} = \bar{\omega}_{K\beta}/\bar{\omega}_{K\alpha} , \tag{2}$$

where

$$\bar{\omega}_K = \sum_{i,f} \omega_K(L_f, M_f) P_{L_f, M_f} P_{L_i, M_i} .$$

In the above equation, $\omega_K(L_f, M_f)$ is the K-shell ($K\alpha$ or $K\beta$) fluorescence yield for L-shell configuration L_f and M-shell configuration M_f. The quantity P_{L_f, M_f} represents the probability of forming (prior to a K-shell transition) the *final* configuration (L_f, M_f) starting from an initial configuration (L_i, M_i), and P_{L_i, M_i} represents the probability of forming the *initial* configuration (L_i, M_i) in the collision. Thus the P_{L_i, M_i} factors can only be determined if the P_{L_f, M_f} factors can be evaluated. This in turn requires a knowledge of all the individual L- and M-shell transition widths for each defect configuration involved, and hence the problem becomes hopelessly complex unless these transition widths happen to be very small compared to the K-shell transition widths, in which case the occurrence of L- and M-shell transitions before K-vacancy decay is very improbable and can be neglected. For intermediate Z elements such as Ti, however, the total L-shell widths for atoms having only a single L-shell vacancy are nearly as large as the total K-shell widths for atoms having only a single K-shell vacancy ($\Gamma_L \sim 0.7\Gamma_K$).[21,22] Therefore it would appear that the above simplification does not apply to the analysis of the present data.

Alternatively, we shall proceed with a less detailed approach based upon several simplifying assumptions in the hopes of extracting information pertaining to the degree of M-shell ionization at the time of K-vacancy decay and its variation with projectile velocity. We begin by expressing the measured $K\beta/K\alpha$ intensity ratio in terms of the fraction $f(i,j)$ of K-vacancy decays which proceed from configuration (i,j);

$$\left(\frac{I_{K\beta}}{I_{K\alpha}}\right)_{\text{expt}} = \sum_{i,j} \omega_{K\beta(i,j)} f_{(i,j)} \Big/ \sum_{i,j} \omega_{K\alpha(i,j)} f_{(i,j)} . \tag{3}$$

Now it has been shown experimentally for a wide range of elements that the fraction of K x rays emitted by atoms having n L-shell vacancies as a result of heavy charged particle collisions can be well represented by the nth term of a binomial series[23-25]

$$\frac{N_n}{N_{\text{tot}}} \simeq \binom{n_L}{n} p_L^n (1-p_L)^{n_L - n} , \tag{4}$$

where

$$\binom{n_L}{n} = \frac{n_L!}{(n_L - n)!\, n!} .$$

Here n_L is the number of L-shell electrons in the ground-state configuration, and p_L may be considered to be a parameter which in effect represents the average probability *per electron* of producing an L-shell vacancy as a result of the combined collision process and subsequent deexcitation processes prior to K x-ray emission. This parameter has been measured for number of cases, including the case of interest here (i.e., carbon ions incident on Ti).[19]

The distribution of L vacancies among the $2s$ and $2p$ subshells will largely depend upon whether or not Coster-Kronig transitions, which shift $2s$ vacancies into $2p$ levels, are energetically allowed for defect configurations. The two limiting cases can be treated as follows:

(i) If Coster-Kronig transitions are allowed for all defect configurations, Eq. (4) can be assumed to give the fraction of K-shell transitions proceeding from configurations involving n $2p$ vacancies.

(ii) If Coster-Kronig transitions are not allowed for any defect configurations, the fraction of K-shell transitions proceeding from a particular L-shell configuration can be assumed to be given by Eq. (4) times a statistical factor representing the probability of obtaining the configuration of interest out of all the possible configurations having the same number of L-shell vacancies. The justification for this is that the form of Eq. (4) implies that the production of a given number of L vacancies, as a consequence of the many complex processes involved, can ultimately be expressed in terms of a simple statistical result. It would therefore seem reasonable to expect that (in the absence of Coster-Kronig transitions) the distri-

bution of L-shell vacancies among the $2s$ and $2p$ subshells would also be statistical. The appropriate statistical factors to be used are given by

$$S_{L(n)} = \binom{n_{2s}}{n_{2s}^*}\binom{n_{2p}}{n_{2p}^*}\Big/\binom{n_L}{n} , \tag{5}$$

where n_{2s} and n_{2p} are the numbers of $2s$ and $2p$ electrons in the ground-state configuration and n_{2s}^* and n_{2p}^* are the numbers of $2s$ and $2p$ electrons which have been removed to obtain the defect configuration ($n_{2s}^* + n_{2p}^* = n$).

We have carried out calculations based upon both assumption (i) and upon assumption (ii), above, in which it has been further assumed that the same prescription for computing the fraction of K-vacancy decays proceeding from a particular L-vacancy configuration can also be applied independently to the M shell. In particular it has been assumed that the fraction of K-vacancy decays proceeding from a configuration involving m M-shell vacancies can be parameterized in terms of the quantity p_M in an analogous fashion to that given by Eq. (4) for L-shell vacancies so that for assumption (ii)

$$f_{(i,j)} = S_{L(n)} S_{M(m)} \binom{n_L}{n} p_L^n (1-p_L)^{n_L - n} \times \binom{n_M}{m} p_M^m (1-p_M)^{n_M - m} , \tag{6}$$

where

$$S_{M(m)} = \binom{n_{3s}}{n_{3s}^*}\binom{n_{3p}}{n_{3p}^*}\binom{n_{3d}}{n_{3d}^*}\Big/\binom{n_M}{m} .$$

In these calculations we have used the scaling procedure suggested by Larkins[20] to compute the $K\alpha$ and $K\beta$ fluorescence yields for the various L- and M-shell vacancy configurations required in Eq. (3). It has already been noted that the degree of accuracy to be expected from the scaling procedure rapidly deteriorates for configurations involving more than two or three L-shell vacancies. Its use here is justified by the fact that previous measurements of p_L values for carbon ions incident on Ti, performed by Li,[19] indicate that the most probable number of L-shell vacancies produced at these velocities is one or less, and that contributions from configurations involving more than three L-shell vacancies are essentially negligible. In addition, we have compared fluorescence yields for defect configurations of Ar atoms computed using the scaling procedure with those obtained by Bhalla[18] from Hartree-Fock-Slater calculations and find a difference of only 17% in the worst case. In the present calculations, the normal Ti K-shell fluorescence yield was taken to be 0.219 as obtained from the semiempirical fit by Bambynek *et al.*[26] and the value of the normal $K\beta/K\alpha$ intensity ratio used was 0.133 as obtained from an average of the photon and bremsstrahlung measurements mentioned previously. Relative K-shell Auger transition probabilities were taken from the calculations of McGuire.[21] The experimental values of p_L for carbon ions incident on Ti, measured previously by Li, were then employed in conjunction with the scaled fluorescence yields to determine the values of p_M [in Eq. (6)] needed to give agreement between the $K\beta/K\alpha$ intensity ratios calculated with Eq. (3) and those obtained experimentally.

The resultant p_M values and average fluorescence yields obtained by assumptions (i) and (ii) are listed in Table VI along with the values of p_L which were used in their determination. The $p_M^{(2)}$ values

TABLE VI. Values of the parameters p_L and p_M, and average fluorescence yields for carbon ions incident on a Ti target. The superscript numbers denote which assumption was used in the evaluation of that particular quantity.

E/M (MeV/amu)	p_L [a]	$p_M^{(i)}$	$p_m^{(ii)}$	$\bar{\omega}_{K\alpha}^{(i)}$	$\bar{\omega}_{K\beta}^{(i)}$	$\bar{\omega}_{K\alpha}^{(ii)}$	$\bar{\omega}_{K\beta}^{(ii)}$
2.35	0.209	0.160	0.109	0.214	0.035	0.211	0.034
3.75	0.146	0.092	0.058	0.209	0.032	0.207	0.032
6.25	0.091	0.065	0.047	0.203	0.029	0.200	0.029
8.33	0.059	0.047	0.037	0.200	0.028	0.197	0.027

[a] Taken from Ref. 19.

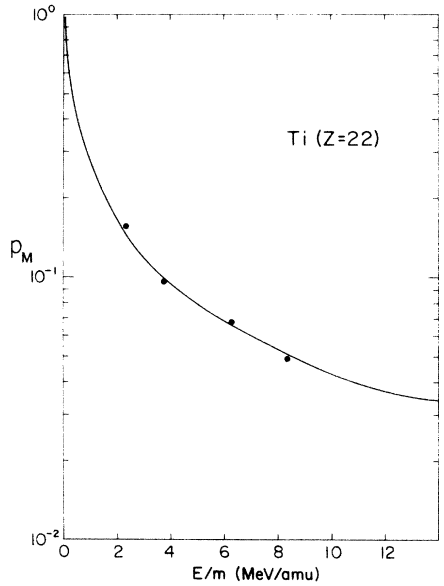

FIG. 6. A comparison of the velocity dependence of the p_M values deduced from the $K\beta/K\alpha$ intensity-ratio measurements for carbon ions incident on Ti with the Gryzinski velocity function for M-shell ionization by Coulomb excitation. The velocity function has been normalized to the data.

are on the average about 30% smaller than the $p_M^{(1)}$ values, while the average fluorescence yields obtained under the two different assumptions only differ on the average by 1.4%. It has been shown previously[4] that the velocity dependence of p_L for light-ion excitation is fairly well characterized by the Gryzinski velocity function[27] for L-shell ionization by direct Coulomb excitation. In Fig. 6, the velocity dependence of $p_M^{(1)}$ is compared with the (normalized) Gryzinski velocity function for Ti M-shell ionization. It is seen that quite good agreement is obtained.

ACKNOWLEDGMENTS

We thank Stanley Sutton for his help in programming the theoretical transition-probability calculations, and T. L. Hardt for assistance with the experimental measurements. Stimulating discussions with Dr. J. S. Hansen contributed to this work and are gratefully acknowledged. Our gratitude goes also to the operations staff of the Texas A&M Cyclotron Institute and in particular to Jack Hernandez for his untiring work in constructing the targets used in these experiments.

---

*Research supported in part by the U. S. Atomic Energy Commission and the Robert A. Welch Foundation.

[1]A. R. Knudson, D. J. Nagel, P. G. Burkhalter, and K. L. Dunning, Phys. Rev. Lett. 26, 1149 (1971).

[2]D. Burch and P. Richard, Phys. Rev. Lett. 25, 983 (1970); Rev. Mod. Phys. 45, 111 (1973), especially p. 163.

[3]R. L. Watson and T. K. Li, Phys. Rev. A 4, 132 (1971).

[4]T. K. Li, R. L. Watson, and J. S. Hansen, Phys. Rev. A 8, 1258 (1973).

[5]C. Rugge, R. L. Watson, and J. B. Wilhelmy (unpublished).

[6]*IAEA Calibrated Gamma Sources, Set 23* (International Atomic Energy Agency, Vienna, 1969).

[7]J. S. Hansen, J. C. McGeorge, D. Nix, W. D. Schmidt-Ott, I. Unus, and R. W. Fink, Nucl. Instrum. Meth. 106, 365 (1973).

[8]V. W. Slivinsky and P. J. Ebert, Phys. Rev. A 5, 1581 (1972).

[9]J. H. McCrary, L. V. Singman, L. H. Ziegler, L. D. Looney, C. M. Edmonds, and C. E. Harris, Phys. Rev. A 4, 1745 (1971).

[10]S. I. Salem, T. H. Falconer, and R. W. Winchell, Phys. Rev. A 6, 2147 (1972).

[11]J. S. Hansen, H. U. Freund, and R. W. Fink, Nucl. Phys. A 142, 604 (1970).

[12]V. D. Mistry and C. A. Quarles, Nucl. Phys. A 164, 219 (1971).

[13]J. H. Scofield, Phys. Rev. 179, 9 (1969).

[14]H. R. Rosner and C. P. Bhalla, Z. Phys. 231, 347 (1970).

[15]C. F. Moore, M. Senglaub, B. Johnson, and P. Richard, Phys. Lett. A 40, 107 (1972).

[16]F. Herman and X. Skillman, *Atomic Structure Calculations* (Prentice-Hall, Englewood Cliffs, N. J., 1963).

[17]C. P. Bhalla, N. O. Folland, and M. A. Hein, Phys. Rev. A 8, 649 (1973).

[18]C. P. Bhalla, Phys. Lett. A 45, 19 (1973).

[19]T. K. Li, Ph.D. thesis (Texas A&M University, 1973) (unpublished).

[20]F. P. Larkins, J. Phys. B 4, 129 (1971).

[21]E. J. McGuire, Phys. Rev. A 2, 273 (1970).

[22]E. J. McGuire, Phys. Rev. A 3, 587 (1971).

[23]D. Burch and H. Swanson, in *Proceedings of the International Conference on Inner Shell Ionization Phenomena*, Conf-720404 (U. S. AEC, 1973), p. 1464.

[24]R. L. Kauffman, J. H. McGuire, P. Richard, and C. F. Moore, Phys. Rev. A 8, 1233 (1973).

[25]R. L. Watson (unpublished).

[26]W. Bambynek, B. Crasemann, R. W. Fink, H-U. Freund, H. Mark, C. D. Swift, R. E. Price, and P. V. Rao, Rev. Mod. Phys. 44, 716 (1972).

[27]M. Gryzinski, Phys. Rev. 138, A336 (1965).